Polymerization of Olefins Through Heterogeneous Catalysis. VII. Particle Ignition and Extinction Phenomena

R. A. HUTCHINSON and W. H. RAY*Department of Chemical Engineering, University of Wisconsin, Madison, Wisconsin 53706

Synopsis

The possibility of multiple steady states for a polymer particle is examined for propylene and ethylene, liquid and gas phase polymerizations. It is shown that multiple steady states should not occur in conventional diluent slurry polymerizations, but are always a possibility for gas phase and bulk propylene slurry reactions. Simulations to determine particle temperatures as a function of particle diameter show that polymer melting is predicted immediately upon catalyst injection for many cases in a gas phase reactor and for some cases in bulk polymerization. The practical implications of this result are discussed.

INTRODUCTION

In catalyzed olefin polymerization, one of the most critical design problems is removal of the heat of polymerization. This is especially true for gas phase processes, where poor heat removal can lead to agglomeration of particles, poor mixing and, ultimately, process breakdown. The design of reactor heat removal systems is discussed extensively in the patent literature for both stirred beds (e.g., Refs. 1 and 2) and fluidized beds (e.g., Refs. 3–6). However, even with good macroscopic reactor heat removal, hotspots and polymer buildup on internal reactor surfaces still occur. Two previous papers in this series[7,8] address this problem through an investigation of internal and external boundary layer heat and mass transfer effects for a growing polymer particle. It was found that while internal temperature gradients in the polymer particle could exist under extreme conditions (i.e., large catalyst particles, highly active catalyst, etc.), the largest temperature gradients arise in the external boundary layer surrounding the particle. In the previous treatment,[7] the principal results concerning external temperature gradients were calculated assuming a fixed catalyst productivity rate independent of particle temperature rise. This is a good assumption for those catalysts with activation energies near zero. However, a number of catalysts in use show activation energies in the range 3–15 kcal/mol. In this paper we investigate the external particle temperature gradients when the catalyst has an activation in the above range for temperatures up to the polymer particle softening temperature. By including this effect in the model, the possibility of multiple steady states for a polymer particle becomes apparent. Here we describe the possibilities for particle multiplicity (i.e., ignition and extinction) for slurry,

*Author to whom correspondence should be addressed.

Journal of Applied Polymer Science, Vol. 34, 657–676 (1987)
© 1987 John Wiley & Sons, Inc. CCC 0021-8995/87/020657-20$04.00

TABLE I
Parameters and Operating Conditions for Polymerization

	Ethylene		Propylene		
	Hexane slurry	Gas phase	Heptane slurry	Gas phase	Bulk slurry
M_b (mol/cm^3)	0.002	0.001	0.004	0.001	0.0095
T_b (K)	353	353	343	343	333
$(-\Delta H)$ (cal/mol)	22,700	25,700	20,500	24,800	24,800
E (cal/mol)	10,000	7000	10,000	7000	7,000
k_f (cal/cm s K)	2.3×10^{-4}	7.0×10^{-5}	2.5×10^{-4}	5.0×10^{-5}	1.8×10^{-4}
ρ (g/cm^3)	0.576	0.028	0.54	0.042	0.40
D_b (cm^2/s)	1.0×10^{-4}	6.0×10^{-3}	8.0×10^{-5}	4.0×10^{-3}	—
C_p (cal/g K)	0.604	0.44	0.671	0.40	0.82
μ (g/cm s)	1.49×10^{-3}	1.2×10^{-4}	1.35×10^{-3}	1.0×10^{-4}	1.0×10^{-3}
ρ_c (g/cm^3)	1.9	1.9	1.9	1.9	1.9

gas phase, and liquid pool polymerizations, and interpret the results in terms of observed industrial phenomena. Two classes of conditions are considered; reactions which have boundary layer mass transfer (conventional slurry and multicomponent gas phase reactions), and those for which no concentration gradient would be expected (pure component gas phase and propylene bulk slurry reactions).

PHYSICAL PROPERTIES AND OPERATING CONDITIONS

The physical properties and operating conditions used in this analysis are consistent with those used in previous papers from this series,[7,8] and are shown in Table I. Cases examined are ethylene in hexane, propylene in heptane, and bulk propylene liquid phase polymerizations, as well as ethylene and propylene gas phase polymerizations. Concentrations and temperatures listed in Table I are typical values for industrial reactors. As noted in Ref. 7, the diffusivity coefficients given for gas phase processes are the self-diffusion coefficients for the olefin monomers; these provide a conservative estimate for diffusion through comonomer, inerts, or hydrogen. The physical properties for liquid propylene are taken from Ref. 9, with the thermal conductivity estimated using a correlation taken from Ref. 10.

Throughout the analysis, physical properties are assumed to be constant across the particle boundary layer, even if the temperature gradient is significant. At first glance, this may seem to be a poor assumption, since temperature gradients of greater than 1000°C are predicted by some of the simulations. However, the question addressed in this study is whether or not the polymer particle will reach its melting point; thus the region of interest is only up to the temperature at which the polymer melts—a span of only $\simeq$ 60°C. Therefore, the assumption of constant physical properties is adequate for the present analysis.

The correlations for heat and mass transfer coefficients were also reviewed in Ref. 7; this paper mainly uses the Ranz–Marshall correlation[11] for a single sphere moving with relative velocity u:

$$\mathrm{Sh} = 2.0 + 0.6(\mathrm{Sc})^{1/3}(\mathrm{Re})^{1/2}$$

$$\mathrm{Nu} = 2.0 + 0.6(\mathrm{Pr})^{1/3}(\mathrm{Re})^{1/2} \qquad (1)$$

where

$$\mathrm{Sh} = \frac{k_s d_p}{D_b}, \quad \mathrm{Nu} = \frac{h d_p}{k_f}, \quad \mathrm{Sc} = \frac{\mu}{\rho D_b}, \quad \mathrm{Pr} = \frac{\mu C_p}{k_f}, \quad \mathrm{Re} = \frac{\rho u d_p}{\mu},$$

This correlation was chosen because it leads to the theoretical single-sphere asymptote of 2, assuming an infinite boundary layer around the particle. However, Sh and Nu numbers of less than 2 have been observed experimentally, especially in stagnant regions of high particle concentration where particle–particle interactions become important.[7] One correlation which looks at this explicitly is the Nelson–Galloway correlation,[12] which has an added parameter, ϵ, the fluid fraction of the concentrated particle–fluid system:

$$\mathrm{Sh \text{ or } Nu} = \frac{2\zeta + \tanh(\zeta)\left[\dfrac{2\zeta^2(1-\epsilon)^{1/3}}{\left[1-(1-\epsilon)^{1/3}\right]^2} - 2\right]}{\dfrac{\zeta}{\left[1-(1-\epsilon)^{1/3}\right]} - \tanh(\zeta)} \tag{2}$$

where

$$\zeta = \left[(1-\epsilon)^{-1/3} - 1\right] 0.3\,\mathrm{Re}^{1/2}(\mathrm{Sc \text{ or } Pr})^{1/3}$$

As in Ref. 7, the relative particle velocity is an input parameter for gas phase simulations, but is calculated assuming a free-settling condition in slurry reactors.

CASE 1: MULTICOMPONENT FLUID PHASE

Figure 1 shows a growing polymer particle of diameter d_p and surface area A_p which has grown up from a catalyst particle of original diameter d_c and volume V_c. Note that both monomer and temperature have a gradient from the bulk phase (M_b, T_b) through the boundary layer to the surface of the growing particle (M_s, T_s). Because the external temperature gradients dominate, in this paper we shall neglect internal temperature gradients. Although internal gradients would play a role under extreme conditions, it is thought that multiplicity phenomena below the particle softening point are governed by the external boundary layer gradients. Internal concentration gradients are also neglected in this analysis, which is certainly a good assumption for gas phase polymerization with current catalysts.[8] However, for multicomponent liquid phase polymerization, internal concentration gradients would be significant and would limit reaction rate. This will be discussed in more detail below.

The steady state mass balance for the polymer particle is

$$A_p k_s (M_b - M_s) = V_c R_p \tag{3}$$

where R_p is the rate of polymerization in mol/cm^3 s and k_s is the mass transfer coefficient. The corresponding energy balance is

$$A_p h (T_b - T_s) = (-\Delta H) V_c R_p \tag{4}$$

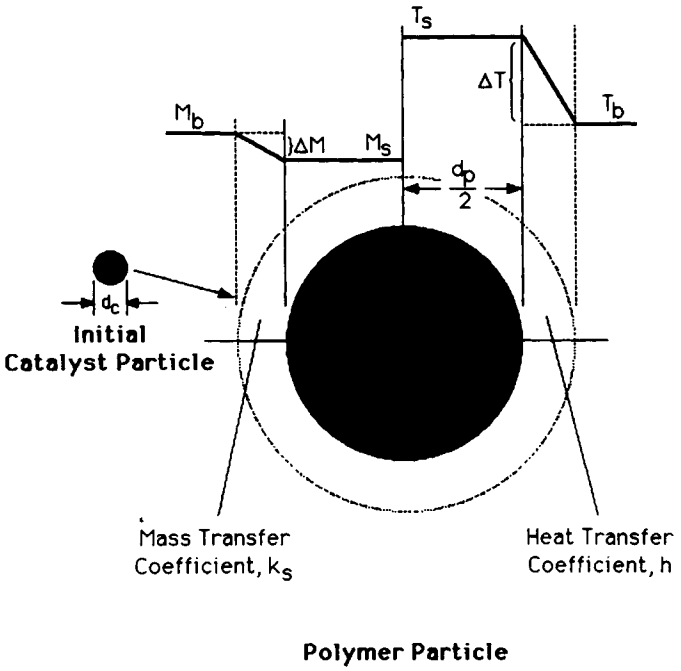

Fig. 1. Idealized picture of the growing polymer particle showing the external boundary layer.

Simultaneous solution of (3) and (4) gives the monomer concentration at the particle surface:

$$M_s = M_b - \frac{h(T_s - T_b)}{k_s(-\Delta H)} \tag{5}$$

This expression is submitted into the reaction rate expression,

$$R_p = (k_p C^*)_b M_s \exp[E/R(1/T_b - 1/T_s)] \tag{6}$$

to give

$$R_p = (k_p C^*)_b [M_b - h(T_s - T_b)/(k_s(-\Delta H))] \exp[\gamma(1 - 1/y_s)] \tag{7}$$

where $y_s = T_s/T_b$ and $\gamma = E/RT_b$ are dimensionless parameters. The final step involves substituting (7) into the energy balance (4), which leads to the expression

$$F(y_s) = K = [(1 + \beta - y_s)/(y_s - 1)] \exp[\gamma(1 - 1/y_s)] \tag{8}$$

where K and β are dimensionless parameters defined as

$$K = \frac{A_p k_s}{V_c (k_p C^*)_b}, \qquad \beta = \frac{(-\Delta H) k_s M_b}{h T_b}$$

By definition of the Sherwood and Nusselt numbers, the expression for β becomes

$$\beta = \left(\frac{D_b M_b(-\Delta H)}{k_f T_b}\right)\left(\frac{\mathrm{Sh}}{\mathrm{Nu}}\right) \tag{9}$$

Similarly, expressing the rate of polymerization in terms of the observed rate in g/(g cat)(hr) at T_b,

$$R_p = (k_p C^*)_b M_b = R_{ob}\rho_c/(3600(\mathrm{MW})_m)$$

leads to the following expression for K:

$$K = \frac{21{,}600 d_p(\mathrm{MW})_m M_b \mathrm{Sh} D_b}{d_c^3 R_{ob}\rho_c} \tag{10}$$

Implicit in the above analysis is that the pseudo-steady state assumption is valid; i.e., the accumulation terms of the energy and mass balance equations are negligible. It is easy to show that this assumption is justified, because the characteristic time constants for equilibration of the mass and energy balances are only a small fraction of a second.

In order to analyze for multiplicity of the polymer particle, eq. (8) is the appropriate form since Luss[13] has shown that a necessary condition for multiple steady states is

$$\gamma\beta > 4(1 + \beta) \tag{11}$$

If this condition is met, then multiple steady states will occur if and only if

$$F(y_{\min}) \leq K \leq F(y_{\max}) \tag{12a}$$

where

$$y_{\max,\min} = \frac{\gamma(2 + \beta) \pm \{\gamma\beta[\gamma\beta - 4(1 + \beta)]\}^{1/2}}{2(1 + \beta)} \tag{12b}$$

Notice that the necessary condition (11) is independent of catalyst activity, involving only the parameters γ and β; thus it can be used to perform a preliminary analysis on different reactor types. If (11) is satisfied, then (12) must be examined to see if multiple steady states will exist for the range of catalyst activities of interest.

Conventional Diluent Slurry Polymerization

First let us consider conventional slurry polymerization, taking place in an inert hydrocarbon diluent. Substituting the physical properties and parameters listed in Table I into (11) leads to the necessary condition that $\beta > 0.375$, or Sh/Nu > 4.9 for multiple steady states to be even possible in a propylene–heptane slurry polymerization. For ethylene–hexane slurry polymerization, the necessary condition is that Sh/Nu > 7.0.

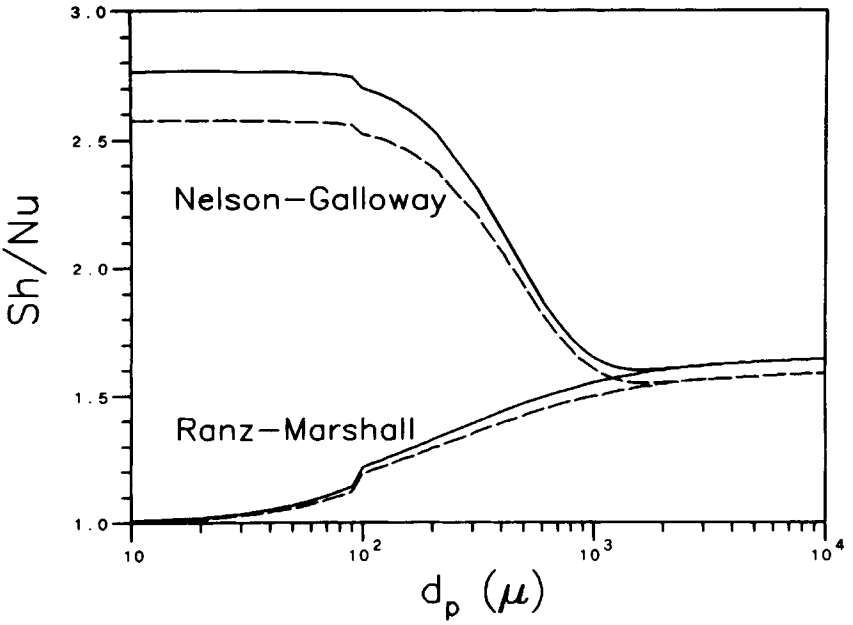

Fig. 2. Values of Sh/Nu for ethylene slurry (---) and propylene slurry (——) polymerizations for Ranz–Marshall and Nelson–Galloway ($\epsilon = 0.6$) correlations.

To examine whether these conditions can be met, values of Sh and Nu were evaluated over a particle range 10–10,000 μm using the Ranz–Marshall and Nelson–Galloway correlations mentioned above. Figure 2 shows that for both ethylene and propylene slurries the ratio of the two dimensionless numbers is never greater than 2, using the Ranz–Marshall correlation, and has a maximum of 2.75 at the start of the reaction according to the Nelson–Galloway correlation with $0.6 \leq \epsilon \leq 1.0$. Even when assuming an unreasonably high activation energy of 15 kcal/mol, the necessary condition (11) shows that Sh/Nu must be greater than 3 for multiple steady states to be possible. As seen above, for the practical particle size range, Sh/Nu can never reach this value according to the correlations used. It is useful to note that any neglected internal particle mass transfer resistance would reduce the effective value of Sh/Nu, making the possibility of multiple steady states even less likely. Thus it can be concluded that, independent of catalyst activity, multiple steady states should not be possible for diluent slurry polymerizations.

Multicomponent Gas Phase Polymerization

Heat and mass transfer in gas phase polymerization can be contrasted with that in slurry phase: there is reduced mass transfer resistance (higher diffusivity) and increased heat transfer resistance (lower thermal conductivity) in gas phase. For the values listed in Table I, the multiplicity condition (11) reduces to Sh/Nu > 0.11 for the possibility of multiple steady states to occur for either ethylene or propylene polymerization in gas phase. Although actual values of Sh and Nu depend on the relative velocity of the polymer particles in the fluid, it is always true that the ratio of Sh/Nu is greater than 0.5 for

the range of velocities encountered in gas phase polymerization. Thus, for gas phase polymerizations, this preliminary analysis shows that regardless of catalyst activity, multiple steady states are always a possibility. The region for which they exist depends on catalyst activity, particle size, and particle velocity, as discussed below.

To examine the region of multiplicity during the growth of a polymer particle, the solution method is as follows: At each polymer particle diameter the Nu and Sh numbers are estimated, the multiple steady state conditions (11, 12) are checked, and the steady state solutions to eqs. (4) and (7) are found. Thus a plot of ΔT, the boundary layer temperature gradient, vs. d_p can be constructed, showing the region of multiplicity during particle growth. These solutions are quasi-steady states which result because particle growth occurs over a period of hours while particle dynamics are on the order of seconds. Thus the particle temperature rise constantly changes in a quasi-steady fashion throughout the polymerization as the polymer particle grows.

As an example, consider a catalyst particle of diameter 60 μm with an observed rate of polymerization of 4000 g/(g cat)(h) at 70°C in a fluidized bed (relative gas–solid velocity = 20 cm/s). Using parameters from Table I, the temperature rise shown in Figure 3 was generated for both ethylene and propylene gas phase polymerizations. There are two stable steady state branches—the upper one at a ΔT above 1000°C, and the lower one which starts at a ΔT of $\simeq$ 40°C and decreases. The upper steady state would obviously result in polymer melting and agglomeration, while the lower branch is tolerable. Notice that the lower branch does not start until the

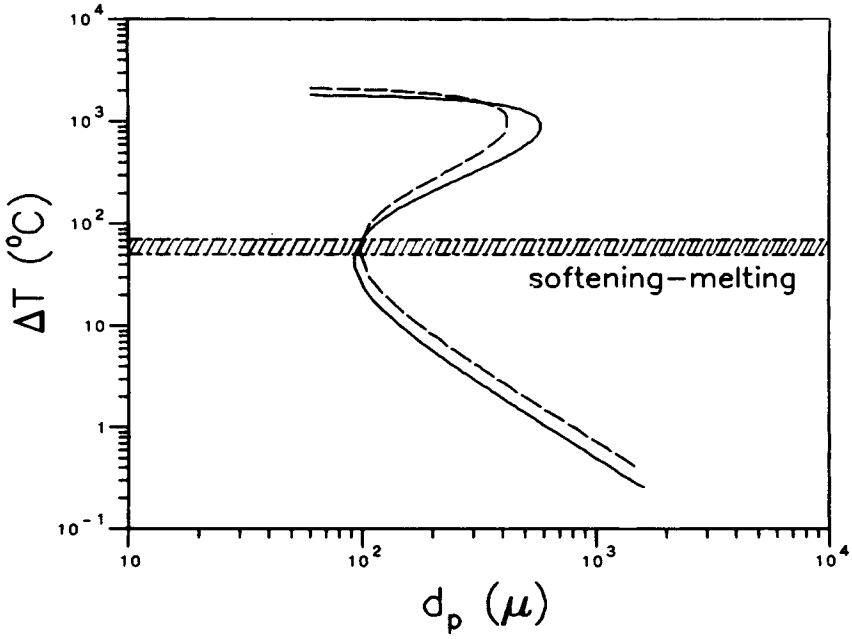

Fig. 3. Particle temperature rise for ethylene (---) and propylene (——) gas phase polymerizations. R_{ob} = 4000 g/(g cat)(h) at bulk conditions, d_c = 60 μm, u = 20 cm/s, Ranz–Marshall correlation.

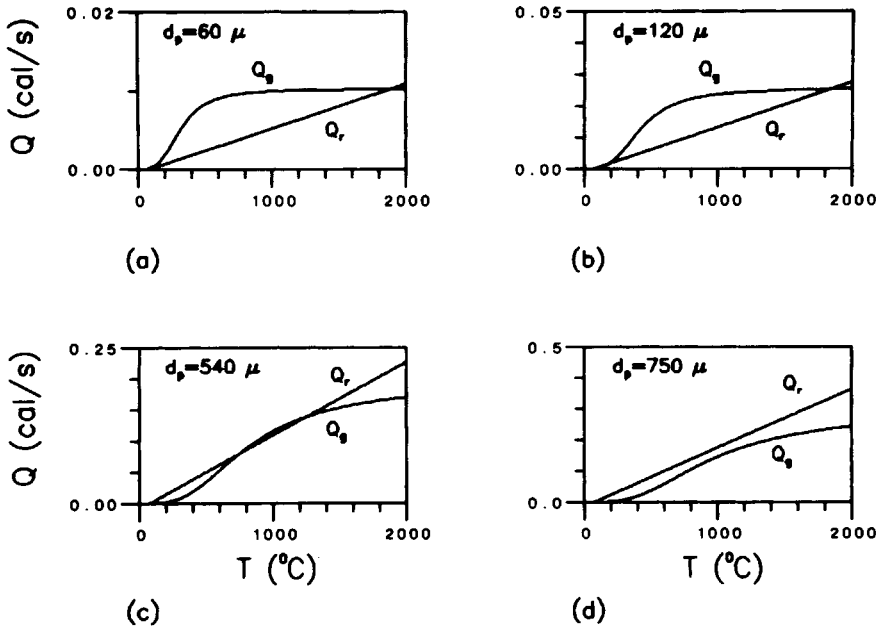

Fig. 4. Heat removal and generation curves as a function of surface temperature at various particle diameters for propylene gas phase polymerization (same conditions as Fig. 3).

particle has grown to a diameter of 92 μm—a replication factor of 1.5 over the original catalyst particle size. Before this diameter is reached, only the upper steady state exists. Thus the simulation predicts that, immediately after catalyst injection, there would be sticking problems in the reactor due to melting of these particles.

Figure 4 shows heat removal and heat generation diagrams at specific diameters throughout the propylene polymerization simulation of Figure 3. At the start of the reaction, where $d_c = d_p = 60$ μm, there is only one intersection point between the two curves [Fig. 4(a)]; until the temperature of 1850°C is reached, the heat removed is always less than the heat generated by polymerization. When the particle has grown to $d_p = 120$ μm, the slope of the heat removed curve has increased (due to increased surface area) so that three intersection points occur: stable solutions at 80 and 1800°C, and an unstable intermediate point [Fig. 4(b)]. Multiple steady state solutions are present even at a diameter of 540 μm [Fig. 4(c)]; after that point the particle surface area is large enough so that the heat removed is greater than the heat generated at all points except at the lower steady state, as shown in Figure 4(d).

This result has interesting implications. At the start of a gas phase polymerization under these conditions, the only steady state solution which exists results in particle melting. To explore the range of conditions at which this is true, further simulations were carried out, looking at the effect of various parameters on the steady state solution diagrams. The remainder of the simulations are for propylene polymerizations only; however, as Figure 3 shows, the results for ethylene reactions are very similar.

The series of simulations shown in Figure 5 examine the combined effect of catalyst diameter and activity on the steady state solution diagrams for

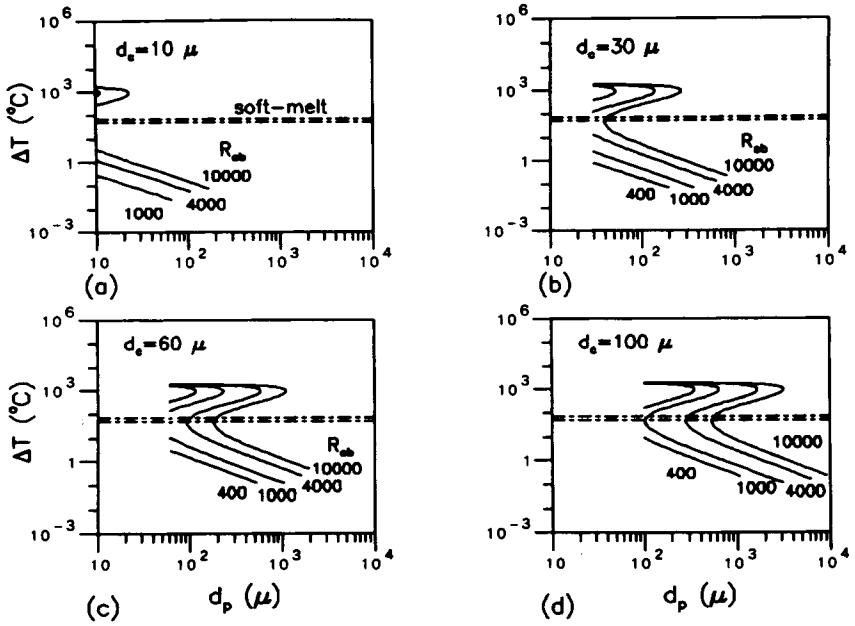

Fig. 5. Particle temperature rise for propylene fluidized bed gas phase polymerizations at varying bulk catalyst activities and catalyst particle sizes. Ranz–Marshall correlation, u = 20 cm/s, R_{ob} in g/(g cat)(h).

propylene polymerization in a fluidized bed. For small catalyst particles [Figs. 5(a) and (b)] of reasonable activity, it is predicted that a lower steady state solution will exist even at the start of the reaction [except for R_{ob} = 10000 g/(g cat)(h) in Fig. 5(b)]; thus no particle melting should occur. However, as the size of the original catalyst particle grows [Figs. 5(c) and (d)] and as activity increases, a region begins to develop for which, early in the reaction, only the upper steady state solution exists and particle melting is predicted. An envelope of this region is shown in Figure 6; this figure can be used to estimate safe regions of operation of a polypropylene fluidized bed reactor. For example, the lower steady state branch begins at a growth factor of 1.5 (d_p = 92 μm) for a catalyst particle of diameter 60 μm and a bulk condition activity of 4000 g/(g cat)(h) while with a bulk condition activity of 10,000 g/(g cat)(h) the lower branch starts at a growth factor of 3.0 (d_p = 180 μm); polymer melting will occur immediately after catalyst injection in both of these cases. At an activity of 1000 g/(g cat)(h) for a 60 μm particle, however, the lower steady state always exists, and melting should not occur. As shown on the figure, this is true for a 60 μm catalyst particle as long as the activity is below ≃ 2200 g/(g cat)(h).

Implicit in this conclusion of "safe" operating regimes is that a large temperature gradient does not already exist when the particles are injected. If a "hot" catalyst particle at 200°C with an observed activity of 1000 g/(g cat)(h) under bulk conditions is injected, the particle will jump to the upper steady state solution, even though a lower temperature solution exists; the initial temperature gradient is sufficient to put the particle in the zone of attraction for the upper steady state. The "zone of attraction" is the region of the solution diagram which is above the intermediate unstable steady state

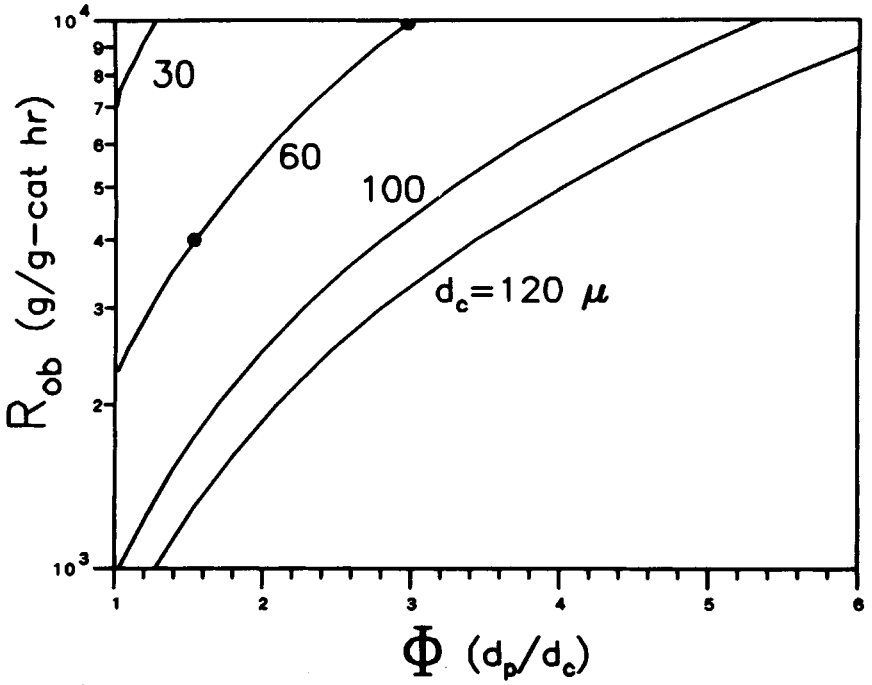

Fig. 6. Predicted operating regions for which polymer melting will occur in a propylene fluidized bed gas phase reactor, using Ranz–Marshall correlation: critical growth factor at which the lower steady state branch begins. R_{ob} is at bulk conditions.

solution. Any particle in this region will be attracted towards the upper stable solution. However, practical industrial conditions make it likely that injection of "hot" catalyst particles would occur only under highly unusual circumstances.

The results in Figures 5 and 6 suggest that the solution to polymer overheating is to decrease catalyst particle diameter. However, there are indications that it is the smaller particles which are preferentially attracted to, and stick to, reactor surfaces.[6,14] At the walls, low fluid velocity leads to reduced heat transfer and an increased chance of particle overheating and agglomeration. A typical value of gas velocity in a fluidized bed is 20 cm/s,[6,15] but, as shown in Figure 7, the danger of overheating increases as the fluidization velocity decreases to the theoretical stagnant asymptote of Nu = Sh = 2. As the velocity decreases from 20 to 0 cm/s, the region at the start of the reaction where particle melting is predicted increases from a particle growth factor of 1.5 to a growth factor of 5.0. Figure 8 illustrates how even a catalyst particle of 30 μm (activity = 4000 g/(g cat)(h) at 70°C) can overheat if it attaches to the wall immediately after injection.

Figures 7 and 8 were constructed assuming a theoretical minimum asymptote of Nu = Sh = 2. However, as mentioned earlier, this is probably not valid for concentrated particle–fluid regions, such as an array of particles stuck on a reactor wall. Thus a few simulations were carried out using the Nelson–Galloway correlation (2). An example case, shown in Figure 9, is for a 10 μm catalyst particle with an observed bulk rate of 4000 g/(g cat)(h) and a local

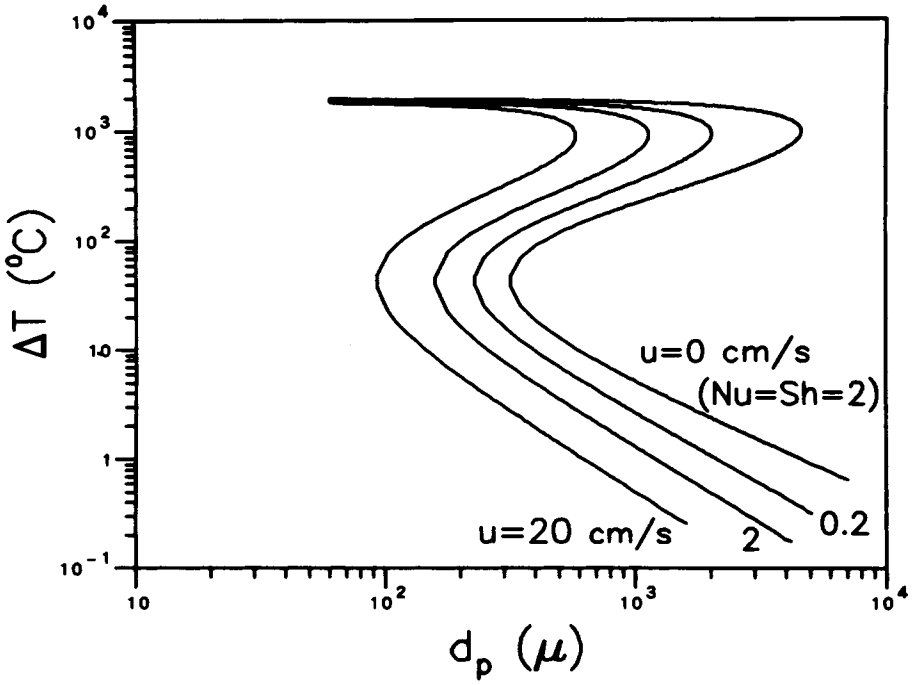

Fig. 7. Effect of fluid–particle velocity on particle temperature rise for a 60 μm catalyst particle with R_{ob} = 4000 g/(g cat)(h) in a propylene gas phase reactor, using the Ranz–Marshall correlation.

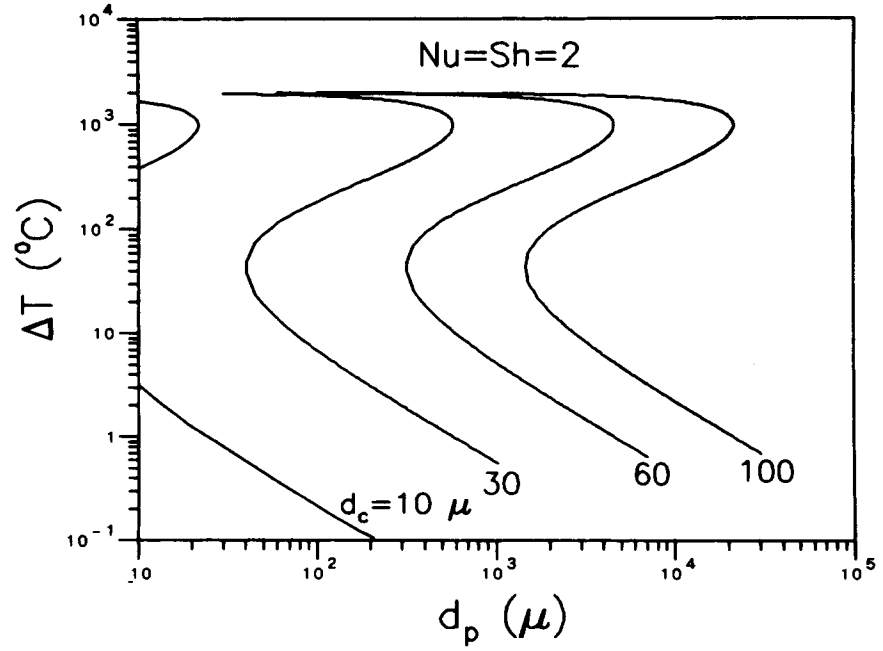

Fig. 8. Particle temperature rise under stagnant conditions (Nu = Sh = 2) in a propylene gas phase reactor. Varying catalyst diameters at R_{ob} = 4000 g/(g cat)(h).

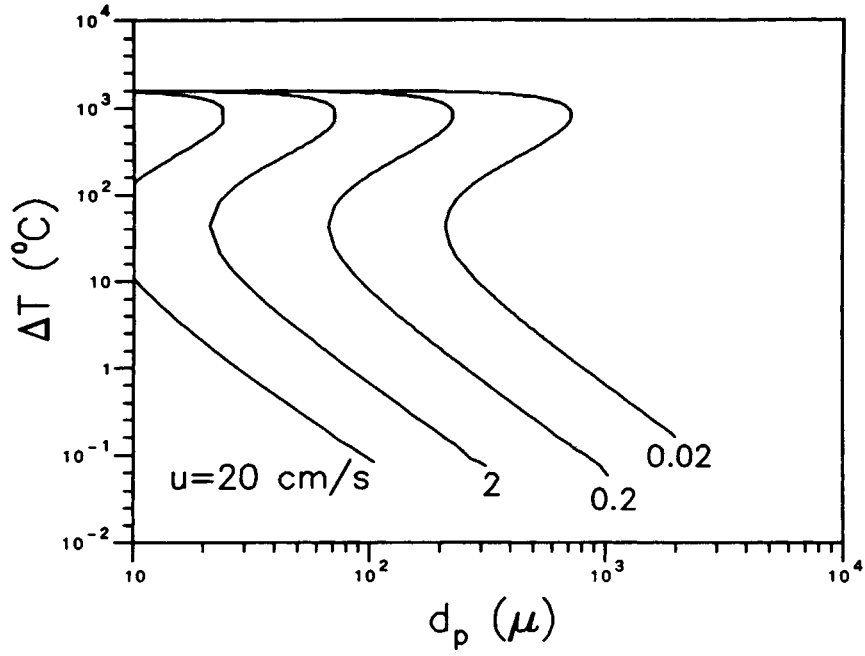

Fig. 9. Effect of particle velocity on particle temperature rise for a 10 μm catalyst particle using the Nelson–Galloway correlation (concentrated particle-fluid conditions). R_{ob} = 4000 g/(g cat)(h), ϵ = 0.6, propylene gas phase reactor.

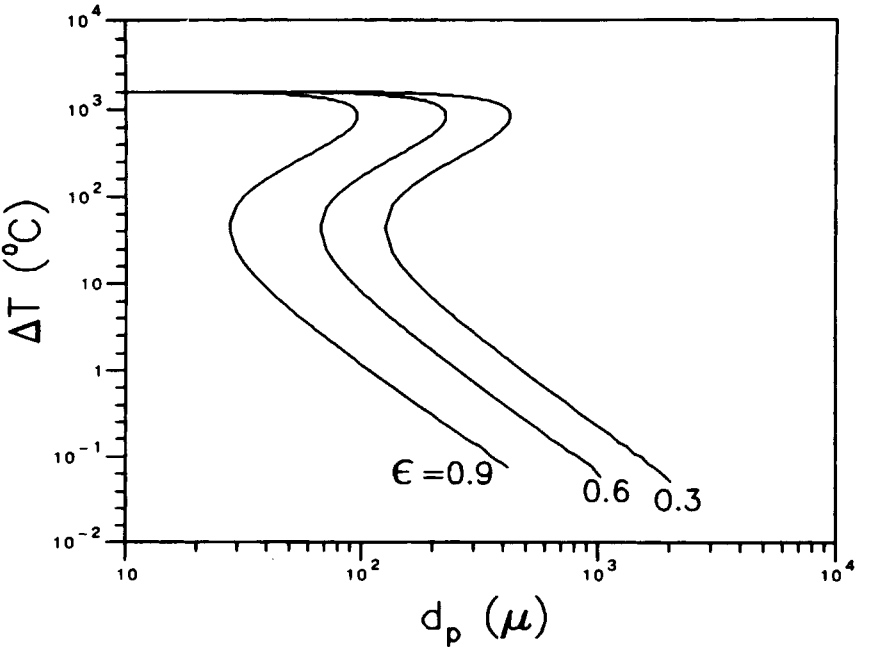

Fig. 10. Effect of fluid fraction in a propylene gas phase reactor on particle temperature rise under relatively stagnant conditions. Nelson–Galloway correlation, u = 0.2 cm/s, R_{ob} = 4000 g/(g cat)(h), d_c = 10 μm.

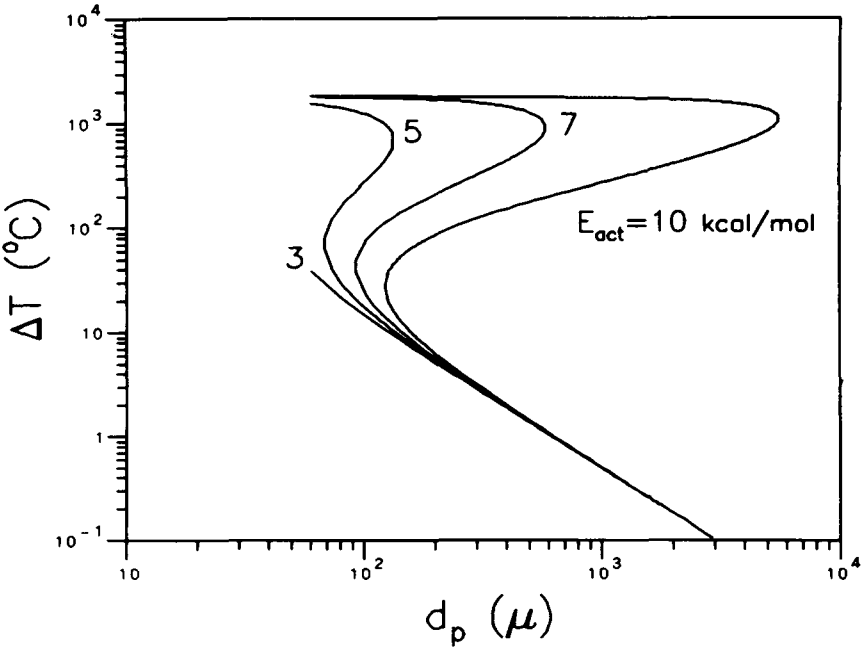

Fig. 11. Effect of activation energy on particle temperature rise for a 60 μm catalyst particle in a propylene gas phase reactor. R_{ob} = 4000 g/(g cat)(h), u = 20 cm/s, Ranz–Marshall correlation.

fluid fraction of 0.6; as the velocity decreases towards zero, the lower steady state solution branch shifts to a larger particle size. The Nelson–Galloway correlation predicts that even particles of 200 μm (a growth factor of 20) will melt if they stagnate in a concentrated particle–fluid region. Figure 10 illustrates the effect of fluid fraction on the steady state solutions in a relatively stagnant region (u = 0.2 cm/s) for a 10 μm catalyst particle. As the solid fraction increases, the lower steady state branch shifts towards larger diameters. These simulations show that if small particles are attracted to reactor surfaces and stagnate, overheating and agglomeration will occur; thus small catalyst particles are not a viable solution to prevent particle overheating.

As mentioned previously, none of the above simulations consider catalyst deactivation. Although olefin catalysts deactivate with time, a more important deactivation process in the consideration of multiple steady states is thermal deactivation. If the number of active sites decrease as the particle temperature increases, the effective activation energy will decrease, making the polymerization rate a weaker function of temperature. This is illustrated in Figure 11, where as the activation energy is decreased from 10 to 3 kcal/mol, the region of multiplicity is eliminated. Such a self-regulating catalyst would be very useful in industry to prevent heat transfer problems, assuming the thermal deactivation is reversible.

CASE 2: A SINGLE COMPONENT FLUID PHASE

The above analysis assumes there is a mass transfer limited concentration gradient across the particle boundary layer. However, for single component

fluids such as gas phase or liquid pool homopolymerizations, mass transfer concentration gradients do not exist, and the assumption can be made that M_s is equal to M_b. For this case, only the energy balance (4) need be considered.

Application of the stability conditions of Luss[13] lead to the following multiple steady state criteria: Multiple steady states will occur if and only if

$$\gamma > 4 \tag{13}$$

and

$$\hat{F}(y_{\min}) \leq \hat{K} \leq \hat{F}(y_{\max}) \tag{14}$$

where

$$\hat{F}(y) = \frac{\exp[\gamma(1 - 1/y)]}{y - 1}$$

$$y_{\max, \min} = \frac{\gamma \pm [\gamma(\gamma - 4)]^{1/2}}{2}$$

$$\hat{K} = \frac{21{,}600 d_p T_b k_f (\mathrm{MW})_m \mathrm{Nu}}{(-\Delta H) d_c^3 R_{ob} \rho_c}$$

For the necessary condition (13) to be satisfied at a bulk temperature of 70°C, it is only necessary to have an activation energy greater than 2.7 kcal/mol; thus the possibility of multiple steady states cannot be ruled out.

Single Component Gas Phase Polymerization

It is interesting to examine the case of single component gas phase polymerization, and compare it to the multicomponent case where mass transfer is not neglected. Figure 12 shows the temperature rise for a 60 μm particle with an observed activity of 4000 g/(g cat)(h) at bulk conditions, with and without a concentration gradient across the boundary layer. The two cases are identical along the lower steady state branch, and differ only at very high temperatures where reaction rates are enormous. If there is no concentration gradient across the boundary layer, it is only possible to have two steady state solutions (the second one is unstable) due to the exponential growth of rate with temperature. For the case of finite mass transfer, it becomes limiting at high temperatures, and the heat generated curve flattens out (see Fig. 4) so that a third solution exists. Both cases lead to virtually the same curves for the lower branch and to the same conclusion: there is a problem with particle overheating and melting early in the particle lifetime. Thus it can be seen that the computations and conclusions of the previous section apply to all gas phase polymerizations, whether they are pure component or multicomponent.

Single Component Bulk Slurry Polymerization

Bulk phase propylene homopolymerization (liquid pool) is another case for which no boundary layer concentration gradient exists. In conventional di-

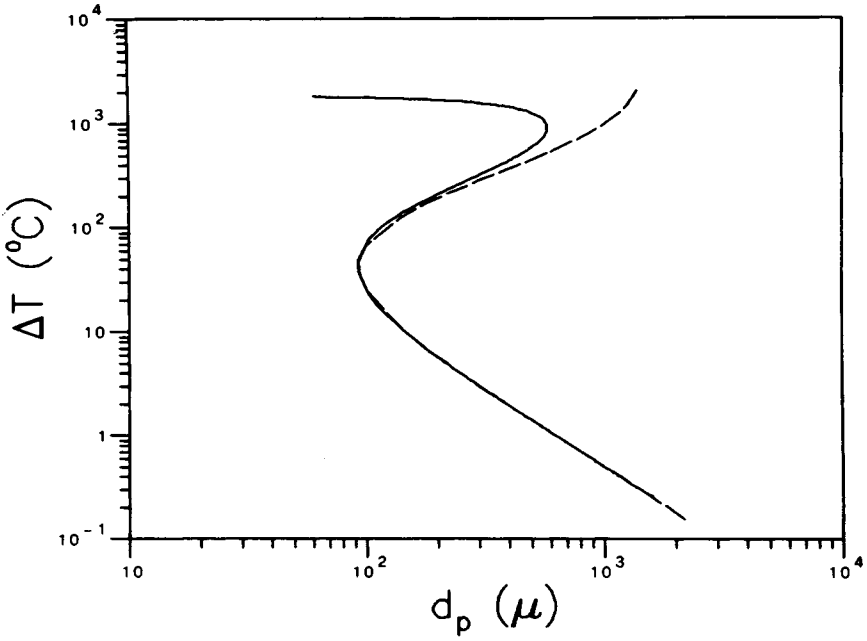

Fig. 12. Comparison of particle temperature rise curves for a propylene gas phase reactor, with (——) and without (---) mass transfer effects. R_{ob} = 4000 g/(g cat)(h), u = 20 cm/s, Ranz–Marshall correlation.

luent slurry polymerizations, the reaction is mass transfer limited due to the presence of hydrocarbon diluent; in liquid pool polymerizations there is no diluent present to cause mass transfer limitations. Also, since monomer concentrations are higher in bulk phase reactors, the reaction rate and heat production per particle are also higher. Thus multiple steady states are possible in liquid pool reactions, even though they are unlikely in conventional slurry reactors. The steady state particle temperature rise for varying catalyst diameters and activities are shown in Figure 13. With an original catalyst size of 30 μm [Fig. 13(a)] there is always a lower steady state solution throughout the particle lifetime, even with a catalyst activity of 10,000 g/(g cat)(h). At an activity of 40000 g/(g cat)(h), however, no solution exists until the particle reaches 70 μm in size. The situation becomes worse as the diameter of the original catalyst particle increases; Figure 13(c) shows that particle melting is predicted immediately upon injection of a 100 μm catalyst particle with a bulk activity of 4000 g/(g cat)(h).

Note that the catalyst activities required for polymer melting in bulk phase reactors are much higher than that in gas phase fluidized beds for the same catalyst particle size; however, the monomer concentrations are almost an order of magnitude higher in the liquid pool reactors. Therefore, for the same catalyst, much higher activities will be observed. No literature could be found discussing particle overheating and melting problems with liquid pool reactors since it is a relatively new process; however, this analysis suggests that it is a problem which might occur.

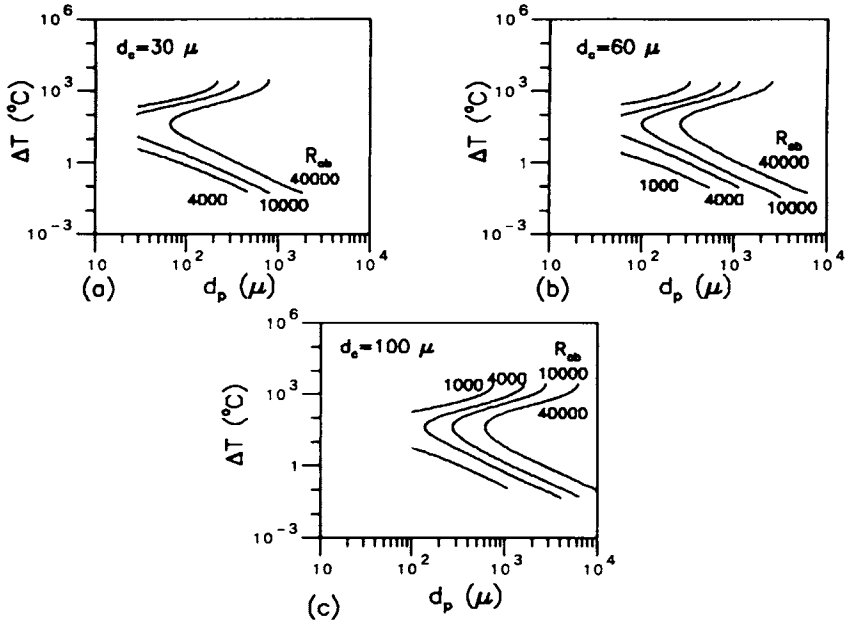

Fig. 13. Particle temperature rise for propylene bulk liquid phase polymerization using Ranz–Marshall correlation. Varying d_c and R_{ob}.

DISCUSSION

The analysis and particle simulations shown above lead to the following "common sense" conclusions for polymerizations where significant temperature gradients can occur:

1. The danger of overheating is the greatest at the start of the reaction, when the polymer particle has a high catalyst volume to surface area ratio. In fact, the simulations predict that massive temperature gradients will occur early in the polymer particle lifetime, due to the absence of the lower steady state solution branch.

2. If the particle enters a stagnant zone in the reactor, decreased fluid–particle velocity leads to decreased heat removal rate and increased chance of polymer melting and sticking.

3. As catalyst activity increases, so do overheating problems. Having a thermally deactivated catalyst helps mitigate this problem, by decreasing the effective activation energy.

A survey of patent literature shows that many ingenious ways of overcoming these problems have been applied to gas phase polymerizations. Many of the patents discuss ways of improving catalyst injection procedures. If the injected catalyst stays together as a lump of particles, overheating is almost guaranteed, since the catalyst concentration is very high compared to the heat transfer area[16–18]; it has the same effect as increasing the catalyst particle diameter. Thus the catalyst is often fed together with other components, either in a gaseous or liquid stream. However, even if the catalyst separates into individual particles after injection, the simulations indicate that overheating will occur. One possible solution to this is to delay the attainment of

full catalyst activity. If full activity of the catalyst particle can be delayed for the first few seconds of the reaction, by the time the catalyst has reached full activity the particle will have a large enough heat transfer surface so that a lower steady state solution exists. A number of patents discuss ways to achieve this.

A 1978 patent to Standard Oil Co. (Indiana)[19] is entitled "Vapor Phase Polymerization with Temporarily Inactive Titanium Catalyst." Their solution involves deactivating the catalyst through use of a base (alcohols are preferred) so that the polymerization ability is reduced by at least 75%. Once inside the reactor, the catalyst is reactivated by aluminum alkyl, which is injected separately. By this method, plugging of the catalyst addition line is avoided. Another possible solution discussed in the same patent involves cooling the carrier liquid which conveys the catalyst into the reactor so as to reduce the catalyst activity. Assuming an activation energy of 7 kcal/mol, if the temperature of the inlet stream is 30°C, activity is decreased by a factor of 4. At a temperature of 0°C, activity is decreased by a factor of 10. However, this solution was rejected as not being economically practical. Also, as pointed out in a Union Carbide patent,[6] having a temperature gradient in the fluidized bed leads to an increased heterogeneity in polymer properties.

BASF patents discuss two different methods of delaying full catalyst activity during the first few critical minutes of reaction. One patent[16] suggests the separate injection of catalyst and cocatalyst at the top and bottom of the stirred bed reactor to prevent polymer sticking problems. Another patent,[20] similar to a Gulf Oil patent,[21] describes a process in which the catalyst is covered by a hydrocarbon wax before injection. The wax melts when the catalyst is introduced into the reactor, but delays catalyst activity sufficiently to avoid heat transfer problems early in polymer particle growth.

A number of dynamic simulations were carried out to examine the effect of delaying full catalyst activity on boundary layer temperature gradients; one case is shown in Figure 14. The example considered is a severe one; a 100 μm catalyst particle with an observed rate of 4000 g/(g cat)(h) at bulk conditions is injected into a fluidized bed. If the catalyst is at full activity at injection time, polymer melting is predicted immediately [see Fig. 5(d)]. However, an activation time constant can be introduced in the form

$$(C^*)_t = (C^*)_\infty [1 - \exp(-t/\tau)] \tag{15}$$

With $\tau = 2$ s, melting still occurs about 1 s after injection (see Fig. 14). However, for $\tau = 5$ s the attainment of full catalyst activity is delayed until the particle has grown past the critical growth factor, and the temperature gradient barely rises above 10°C. Thus Figure 14 shows how even a very small delay in catalyst activation is sufficient to prevent the particles from reaching their upper steady state and melting. It does not take long for a high activity catalyst particle to replicate itself by a factor of 3 or 4.

A second way to avoid overheating of particles early in gas phase polymerization is to increase the heat transfer area from the very beginning of the reaction. Once again patent literature reveals some methods in which this is done. Several patents[3,17,20,22] discuss using a prepolymerization step before proceeding to a gas phase reactor; as shown earlier in this paper, multiple

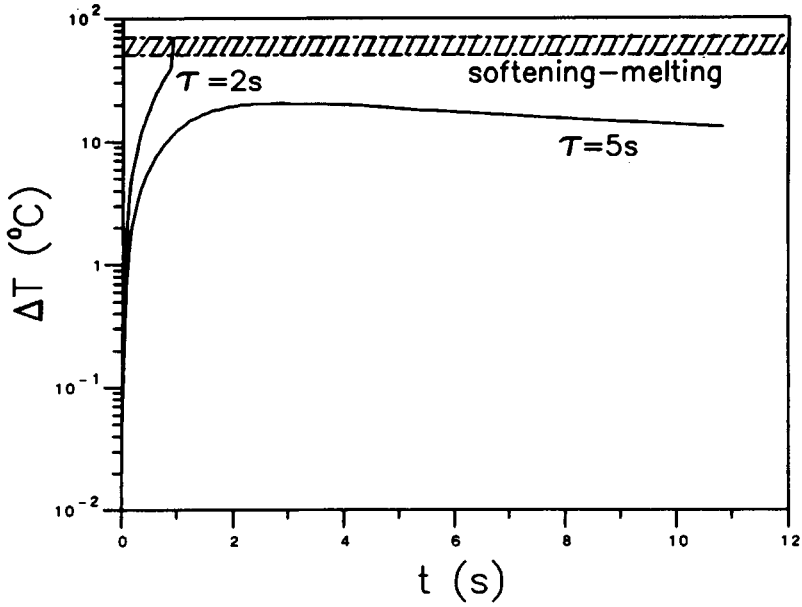

Fig. 14. Effects of delayed catalyst activation on the polymer particle temperature rise for a gas phase polymerization. A dynamic simulation with R_{ob} = 4000 g/(g cat)(h), u = 20 cm/s, d_c = 100 μm, Ranz–Marshall correlation.

steady states do not occur in slurry polymerizations. Other patents discuss using an inert polyolefin support as a catalyst carrier,[23,24] which would also increase the heat transfer surface area.

SUMMARY

The present analysis of particle overheating during olefin polymerization shows that multiple steady states will never be expected in conventional diluent slurry reactors. However, in gas phase reactors there is a large region of particle diameters and catalyst activities at which two stable steady state solutions occur. Simulations show that, in many cases, immediately after catalyst injection the only solution which exists is at a very high temperature so that polymer melting will occur. The same situation may occur in propylene bulk phase polymerization if the catalyst activity is high. It is important to realize that this particle overheating will occur no matter how efficient the macroscale heat removal is in the reactor; the temperature gradient is across the particle boundary layer, and is a steady state condition occurring at constant bulk fluid phase conditions.

These results give a theoretical basis to the wealth of patent literature which deals with methods to counteract overheating problems early in particle lifetime. These methods can be grouped into two major categories: methods which delay the start of full catalyst activity until the danger of overheating is past, and methods which increase the heat transfer surface area through a prepolymerization step or use of a polyolefin support.

APPENDIX: NOMENCLATURE

A_p	polymer particle surface area (cm^2)
C_p	fluid heat capacity (cal/g / K)
d_c	catalyst particle diameter (cm)
d_p	polymer particle diameter (cm)
D_b	bulk diffusivity of monomer in fluid (cm^2/s)
E	activation energy (cal/mol)
h	heat transfer coefficient (cal/cm^2 / s / K)
ΔH	heat of polymerization (cal/mol)
k_f	fluid thermal conductivity (cal/cm / s / K)
k_s	mass transfer coefficient (cm^2 / s)
k_pC^*	rate coefficient at $T_b(s^{-1})$
M_b	bulk monomer concentration (mol/cm^3)
M_s	particle surface monomer concentration (mol/cm^3)
$(MW)_m$	monomer molecular weight (g/mol)
Nu	Nusselt number
Pr	Prandtl number
R	gas constant (1.987 cal/mol / K)
Re	Reynolds number
R_p	rate of polymerization (mol/cm^3 / s)
R_{ob}	observed rate of polymerization (g/g-cat / hr)
Sc	Schmidt number
Sh	Sherwood number
T_b	bulk phase temperature (K)
T_s	particle surface temperature (K)
V_c	volume of catalyst particle (cm^3)
y_s	dimensionless surface temperature
ϵ	fluid fraction of particle–fluid system
μ	fluid viscosity (g/cm / s)
ρ	fluid density (g/cm^3)
ρ_c	apparent catalyst density (g/cm^3)

We are grateful to the National Science Foundation and to the industrial sponsors of the University of Wisconsin Polymerization Reaction Engineering Laboratory for research support. One of the authors (R. A. H.) would also like to thank the National Science and Engineering Research Council of Canada for financial support.

References

1. BASF, U.S. Pat. 3,639,377 (1972).
2. BASF, U.S. Pat. 4,012,573 (1977).
3. Chisso Corp., Eur. Pat. 59,080 (1983).
4. Montedison, U.S. Pat. 3,298,792 (1967).
5. MA Deutschland, U.S. Pat. 3,770,714 (1973).
6. Union Carbide, U.S. Pat. 4,255,542 (1981).
7. S. Floyd, K. Y. Choi, T. W. Taylor, and W. H. Ray, *J. Appl. Polym. Sci.*, **31**, 2231 (1986).
8. S. Floyd, K. Y. Choi, T. W. Taylor, and W. H. Ray, *J. Appl. Polym. Sci.*, **32**, 2935 (1986).
9. R. W. Gallant, *Physical Properties of Hydrocarbons*, Gulf, Houston, 1968, Vol. 1.
10. R. H. Perry and C. H. Chilton, *Chemical Engineers Handbook*, 5th ed., McGraw-Hill, New York, 1973.

11. W. E. Ranz and W. R. Marshall, Jr., *Chem. Eng. Prog.*, **48**, 141 (1952).
12. P. A. Nelson and T. R. Galloway, *Chem. Eng. Sci.*, **30**, 1 (1975).
13. D. Luss, *Chemical Reactor Theory; A Review*, L. Lapidus and N. R. Amundson, Eds. Prentice-Hall, Englewood Cliffs, NJ, 1977, p. 191.
14. W. H. Ray, paper presented at Transition Metal Catalyzed Polymerization Symposium, Akron, OH. 1986.
15. C. Y. Wen and Y. H. Yu, *Chem. Eng. Prog. Symp. Seri.*, **62**, 100 (1966).
16. BASF, U.S. Pat. 3,652,527 (1972).
17. Naphtachimie, U.S. Pat. 3,922,322 (1975).
18. Union Carbide, U.S. Pat. 3,790,550 (1974).
19. Standard Oil Co. (Ind.), U.S. Pat. 4,130,699 (1978).
20. BASF, U.S. Pat. 3,817,970 (1974).
21. Gulf Oil, U.S. Pat. 4,200,712 (1980).
22. Chemisque Werke, U.S. Pat. 4,368,291 (1983).
23. ICI, U.S. Pat. 4,166,167 (1979).
24. Monsanto, U.S. Pat. 3,925,338 (1975).

Received November 18, 1986
Accepted January 13, 1987